

## DEFORMATION FIELD CORRECTION TO PRESERVE TOPOLOGY FOR IMAGE REGISTRATION

SOLÈNE OZERÉ<sup>1</sup>

**Abstract.** In this paper, the author addresses the issue of designing a theoretically well-motivated and computationally efficient method ensuring topology preservation on image-registration-related deformation fields. The model is motivated by a mathematical characterization of topology preservation for a deformation field mapping two subsets of  $\mathbb{Z}^2$ , namely, positivity of the four approximations to the Jacobian determinant of the deformation on a square patch. The first step of the proposed algorithm thus consists in correcting the gradient vector field of the deformation at the discrete level in order to fulfill this positivity condition. Once this step is achieved, it thus remains to reconstruct the deformation field, given its full set of discrete gradient vectors. The author propose to decompose the reconstruction problem into independent problems of smaller dimensions, yielding a natural parallelization of the computations and enabling us to reduce drastically the computational time (up to 80 in some applications). For each subdomain, a functional minimization problem under Lagrange interpolation constraints is introduced and its well-posedness is studied: existence/uniqueness of the solution, characterization of the solution, convergence of the method when the number of data increases to infinity, discretization with the Finite Element Method and discussion on the properties of the matrix involved in the linear system. Numerical simulations based on OpenMP parallelization and MKL multi-threading demonstrating the ability of the model to handle large deformations (contrary to classical methods) and the interest of having decomposed the problem into smaller ones are provided.

## INTRODUCTION

Given two images called Template and Reference, registration consists in determining an optimal diffeomorphic transformation  $\varphi$  such that the deformed Template image is aligned with the Reference. This technique is encountered in a wide range of fields, such as medical imaging, when comparing data to a common Reference frame, when fusing images that have not necessarily been acquired through similar sensors, or when tracking shapes. For images of the same modality, the goal of registration is to correlate the geometrical features and the intensity level distribution of the Reference and those of the Template. For images produced by different mechanisms and possessing distinct modalities, the goal of registration is to correlate the images while maintaining the modality of the Template. The deformation must remain physically and mechanically meaningful, and reflect material properties: self-penetration of the matter (indicating that the transformation is not injective, which is not physically consistent) should be prohibited. When topology preservation is violated, the convexity of the deformed region is infringed, signifying that the images of the corner points of a square patch cross over the diagonal connecting their neighbours. Visually, the deformation field exhibits twists and foldings. This currently occurs when dealing with problems involving large magnitude deformations.

---

<sup>1</sup> Laboratoire de Mathématiques de l'INSA de Rouen, 685 Avenue de l'Université BP08, 76801 Saint-Etienne-du-Rouvray Cedex, France; e-mail: [solene.ozere@insa-rouen.fr](mailto:solene.ozere@insa-rouen.fr)

The necessity of preserving topology arises in brain mapping for instance. It is well-known that the human cortex has a spherical topology (*i.e.*, is homeomorphic to the sphere), so throughout the registration process, this feature must be preserved. Generally speaking, as soon as the shapes to be correlated are homeomorphic, the preservation of orientation must be ensured.

Prior related works addressed this question of maintaining topology. In variational frameworks, the main idea is to control the Jacobian determinant of the deformation, proper measure for the local volume transformation under the considered deformation. The work by Ashburner et al. (see [1], [2] and [3]) and the work by Musse et al. (see [4]) should be mentioned. In [4], the deformation map is modeled as a hierarchical displacement field decomposed on a multiresolution B-splines basis. Topology preservation is enforced by controlling the Jacobian of the transformation. The problem amounts to solving a constrained optimization problem: the residual energy between the target and the deformed source image is minimized under constraints on the Jacobian. This paper is then extended to the 3D case by Noblet et al. (see [5]). The main difference with the proposed approach is that, in our case, the set of feasible transformations is not restricted to a certain class of mappings. In [6], Haber and Modersitzki address the issue of non-parametric image registration under volume-preserving constraints. They propose to restrict the set of feasible mappings by adding a volume-preserving constraint which forces the Jacobian of the deformation to be equal to 1. In [7], the authors pursue in the same direction: they propose to keep the Jacobian determinant bounded, which leads to an inequality-constrained minimization problem.

An alternative to the straight penalization of the Jacobian of the deformation was proposed by Christensen and collaborators. In [8], they introduce a viscous fluid registration model in which objects are viewed as fluids evolving in accordance with the fluid dynamic Navier-Stokes equations. This model is complemented by a regriding technique ensuring positivity of the Jacobian determinant. The method consists in monitoring the values of the Jacobian determinant of the deformation. If the values drop below a defined threshold, the process is reinitialized taking as initialization the last computed deformed Template. However, for problems involving large deformations, numerous regriding steps might be required. Numerically, the resulting deformation field (computed as the composite of intermediate deformations) may not fulfill the topology-preserving conditions, even if the intermediate ones do.

## 1. FIRST STEP : CORRECTION OF THE DEFORMATION

The first step consists in applying the same procedure as the one adopted by Le Guyader et al. in [9]. Given an arbitrary deformation obtained after a registration process, the first step consists in correcting the deformation where the topology is not preserved. To lighten the presentation, the author only provide the key idea of this method and refer the reader to [9] for further details.

Let  $\Omega$  be a connected bounded open subset of  $\mathbb{R}^2$  representing the reference configuration, with Lipschitz boundary  $\partial\Omega$ .

Let  $h : (x_1, x_2) \in \bar{\Omega} \mapsto h(x_1, x_2) = (f(x_1, x_2), g(x_1, x_2))^T$  be the deformation of the reference configuration.

A deformation is a smooth mapping that is orientation-preserving and injective except possibly on  $\partial\Omega$ . Denote by  $u$  the displacement field associated with  $h$ , *i.e.*,  $h = \text{id} + u$ .

The deformation gradient is  $\nabla h : \bar{\Omega} \rightarrow M_2(\mathbb{R})$  defined by  $\nabla h = I_2 + \nabla u$  with  $M_2(\mathbb{R})$  the set of real square matrices of order 2.

The correction algorithm is based on the following proposition which provides a set of conditions to be fulfilled in the discrete setting to ensure topology preservation in the continuous domain.

**Proposition 1.1.** (*From Karaçali and Davatzikos in [10]*)

Let  $\mathcal{C}$  be the class of deformation fields  $h = (f, g)$  defined over a discrete rectangle  $\Omega = [0, 1, \dots, M_1] \times [0, 1, \dots, N_1] \subset \mathbb{N}^2$  for which  $J_{ff}$ ,  $J_{fb}$ ,  $J_{bf}$ ,  $J_{bb}$  are positive for all  $(x, y) \in \Omega$ .

Let  $h = (f, g)$  be a deformation field belonging to  $\mathcal{C}$ . Then its continuous counterpart determined by the interpolation of  $h$  over the domain  $\Omega_C = [0, M_1] \times [0, N_1] \subset \mathbb{R}^2$  using the interpolant  $\Phi$  given by  $\Phi(x, y) = \Psi(x)\Psi(y)$

with

$$\Psi(t) = \begin{cases} 1+t & \text{if } -1 \leq t < 0 \\ 1-t & \text{if } 0 \leq t < 1 \\ 0 & \text{otherwise} \end{cases}$$

preserves topology, with the backward and forward finite difference schemes  $f_x^b, f_x^f, f_y^b, f_y^f$  to approximate the partial derivatives of  $f$  (similarly for  $g$ ) and

$$\begin{cases} J_{ff} = f_x^f(p_1)g_y^f(p_1) - f_y^f(p_1)g_x^f(p_1) \\ J_{bf} = f_x^b(p_2)g_y^f(p_2) - f_y^f(p_2)g_x^b(p_2) \\ J_{fb} = f_x^f(p_3)g_y^b(p_3) - f_y^b(p_3)g_x^f(p_3) \\ J_{bb} = f_x^b(p_4)g_y^b(p_4) - f_y^b(p_4)g_x^b(p_4). \end{cases}$$

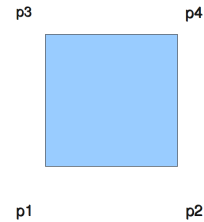


FIGURE 1. Layout of the points on a reference patch.

The general idea resulting from Proposition 1.1 is to balance, at the discrete level and at each node of the grid, the gradients of the displacement vectors by a parameter  $\alpha \in ]0, 1[$ , in order to comply with the above conditions. The existence of such a parameter  $\alpha$  is guaranteed by the intermediate value theorem. Note that applying the correction parameter to the displacement vector field itself would fail to work. It would not guarantee that the obtained discrete Jacobians fulfill these requirements. The algorithm depicted in [9] provides a unique optimal correction parameter per grid node.

## 2. SECOND STEP : DEFORMATION RECONSTRUCTION

The issue to be addressed now lies in the reconstruction of the deformation field, given its discrete set of gradients, with the fewest computations possible (real-time computations should be expected).

Unlike the previous model on this topic [9], formulated as a functional minimization problem on the whole domain  $\Omega$  (-meaning in particular that the computations were made even on regions of the deformation map complying with the orientation-preserving requirement), the author propose to concentrate the computational effort on the subdomains of the deformation grid exhibiting overlaps and to set Lagrange interpolation conditions on the boundary of the subdomains, reproducing more faithfully the physics of the problem. This allows to apply the reconstruction process on each region independently and to reduce significantly the computational cost. In the sequel, assume that  $\mathcal{N}$  nonempty connected bounded open subsets  $\Omega_i$  of  $\Omega$  with Lipschitz boundary,  $i \in \{1, \dots, \mathcal{N}\}$  have been identified (manually for the moment) on which orientation preservation is violated. Then, let introduce a mathematical model of reconstruction, valid for each subdomain  $\Omega_i$ ,  $i \in \{1, \dots, \mathcal{N}\}$ . A  $D^m$ -spline approach is retained (cf. [11]). Generally speaking, the  $D^m$ -splines over an open subset of  $\mathbb{R}^n$  are multidimensional minimizing splines, *i.e.*, functions defined on  $\Omega$  subjected to interpolation or smoothing conditions and that minimize an energy functional involving derivatives of order  $m$ .

### 2.1. Minimization of the energy functional

As said previously  $\forall i \in \{1, \dots, \mathcal{N}\}$ ,  $\Omega_i$  is a nonempty connected bounded open subset of  $\Omega \subset \mathbb{R}^2$  with Lipschitz boundary. Let  $\nu$  be an integer such that  $\nu \in \{1, \dots, \mathcal{N}\}$ . The problem is phrased as a constrained functional minimization problem on a convex subspace of the Hilbert space  $V = H^3(\Omega_\nu, \mathbb{R}^2)$  so that the Sobolev's embedding  $H^3(\Omega_\nu, \mathbb{R}^2) \hookrightarrow C^1(\overline{\Omega_\nu}, \mathbb{R}^2)$  holds (see [12] or [13]). It guarantees, in particular, that the pointwise fitting term dealing with the derivatives of the unknown is well-defined. Thus, it is possible to rebuild a

smoother-than-required deformation field but retain only the values of the deformation components obtained at the grid nodes (centers of gravity of the pixels). Before depicting the model, let us introduce some fundamental mathematical notions that will be useful to state the functional minimization problem.

For any  $\gamma = (\gamma_1, \gamma_2) \in \mathbb{N}^2$ , let's write  $|\gamma| = \gamma_1 + \gamma_2$  and  $\partial^\gamma = \frac{\partial^{|\gamma|}}{\partial x_1^{\gamma_1} \partial x_2^{\gamma_2}}$ . Recall that:

$$\|v\|_{\mathbb{H}^3(\Omega_\nu, \mathbb{R}^2)}^2 = \sum_{|\gamma| \leq 3} \int_{\Omega_\nu} \langle \partial^\gamma v, \partial^\gamma v \rangle_2 dx_1 dx_2, \quad \text{and} \quad |v|_{\mathbb{H}^3(\Omega_\nu, \mathbb{R}^2)}^2 = \sum_{|\gamma|=3} \int_{\Omega_\nu} \langle \partial^\gamma v, \partial^\gamma v \rangle_2 dx_1 dx_2,$$

where  $\langle \cdot, \cdot \rangle_2$  denotes the Euclidean scalar product in  $\mathbb{R}^2$ . For the sake of clarity, we recall the general definition of a  $P$ -unisolvent set.

**Definition 2.1.** (see [11])

For any  $l \in \mathbb{N}$ , we denote by  $P_l$  the space of polynomial functions defined over  $\mathbb{R}^n$  of degree  $\leq l$  with respect to the set of variables, and for any  $l \in \mathbb{N}$  and for any nonempty connected open subset  $\Omega$  in  $\mathbb{R}^n$ , by  $P_l(\Omega)$  the space of restrictions to  $\Omega$  of the functions in  $P_l$ . A set  $A = \{a_1, \dots, a_N\}$  of  $N$  points of  $\mathbb{R}^n$  is  $P_l$ -unisolvent if  $\forall \{\alpha_1, \dots, \alpha_N\} \subset \mathbb{R}, \exists! \Psi \in P_l, \forall i \in \{1, \dots, N\}, \Psi(a_i) = \alpha_i$ .

Let  $A = \{a_i\}_{i=1, \dots, N}$  be a set of  $N$  points of  $\overline{\Omega_\nu}$  containing a  $P_1$ -unisolvent subset. In this application, the set  $A$  is made of the coordinates of the image pixels included in  $\overline{\Omega_\nu}$ .

Let also  $\{\omega_i\}_{i=1, \dots, N}$  be the set of  $N$  Jacobian matrices of the deformation given at  $\{a_i\}_{i=1, \dots, N}$ . This set is made of the corrected gradient vectors of the deformation obtained at the correction step of the algorithm. At last, let  $\{b_i\}_{i=1, \dots, l}$  be  $l$  points of  $\overline{\Omega_\nu}$  where the discrete gradient vectors of the deformation have been unaltered (so the deformation is unchanged). In all our applications, these points will belong to the boundary  $\partial\Omega_\nu$  of  $\Omega_\nu$ . We set Lagrange interpolation constraints at these points. It means that if  $h$  denotes the unaltered deformation and  $v$  denotes the unknown deformation of the minimization problem, we must have:  $\forall i \in \{1, \dots, l\}, v(b_i) = h(b_i)$ . Let  $K$  be the set defined by  $K = \{v \in \mathbb{H}^3(\Omega_\nu, \mathbb{R}^2), \beta(v) = \eta\}$ , with

$$\beta : \begin{cases} \mathbb{H}^3(\Omega_\nu, \mathbb{R}^2) \rightarrow \mathbb{R}^{2l} \\ v \mapsto \beta(v) = (v(b_1), \dots, v(b_l))^T \end{cases}$$

and  $\eta = (h(b_1), \dots, h(b_l))^T$ . The convex set  $K$  is closed as the reciprocal image of a closed set by a continuous mapping. The approximation problem can be stated as follows: given the set of  $N$  Jacobian matrices defined at  $\{a_i\}_{i=1, \dots, N}$ , search for  $v$  sufficiently smooth such that  $\forall i \in \{1, \dots, N\}$ , the Jacobian matrix  $Dv$  evaluated at  $a_i$  is close to  $w_i$  and such that  $\forall i \in \{1, \dots, l\}, v(b_i) = h(b_i)$ . In this purpose, we need the following additional notations. We denote by  $\rho$  the operator defined by:

$$\rho : \begin{cases} \mathbb{H}^2(\Omega_\nu, \mathbb{R}^{2 \times 2}) \rightarrow (\mathbb{R}^{2 \times 2})^N \\ v \mapsto \rho(v) = (v(a_1), v(a_2), \dots, v(a_N))^T \end{cases} \quad (1)$$

The problem is then cast as an optimization one by means of functional  $\mathcal{J}_\epsilon$  defined by:

$$\mathcal{J}_\epsilon : \begin{cases} \mathbb{H}^3(\Omega_\nu, \mathbb{R}^2) \rightarrow \mathbb{R} \\ v \mapsto \langle \rho(Dv) - w \rangle_N^2 + \epsilon |v|_{\mathbb{H}^3(\Omega_\nu, \mathbb{R}^2)}^2, \end{cases}$$

with  $\epsilon > 0$  a tuning parameter and with  $w = (w_1, w_2, \dots, w_N)^T \in (\mathbb{R}^{2 \times 2})^N$ . The operator  $\langle \cdot, \cdot \rangle_N$  is defined as follows:  $\forall \xi \in (\mathbb{R}^{2 \times 2})^N, \forall \eta \in (\mathbb{R}^{2 \times 2})^N, \langle \xi, \eta \rangle_N = \sum_{i=1}^N \sum_{j=1}^4 \xi_{ij} \eta_{ij}$  and  $\langle \xi \rangle_N = \langle \xi, \xi \rangle_N^{\frac{1}{2}}$ . The first term of functional  $\mathcal{J}_\epsilon$  ensures closeness to the data while the second component is a regularizing component. We consider the following minimization problem :

$$\begin{cases} \text{Search for } \sigma_\epsilon \in K \text{ such that} \\ \forall v \in K, \mathcal{J}_\epsilon(\sigma_\epsilon) \leq \mathcal{J}_\epsilon(v). \end{cases} \quad (2)$$

It can be noticed that minimizing  $\mathcal{J}_\epsilon$  with respect to  $v$  is equivalent to minimizing:

$$\langle \rho(Dv) \rangle_N^2 - 2\langle \rho(Dv), \omega \rangle_N + \epsilon |v|_{\mathbf{H}^3(\Omega_\nu, \mathbb{R}^2)}^2.$$

From now on, we thus denote by  $\mathcal{J}_\epsilon$  the new functional :

$$\mathcal{J}_\epsilon : \begin{cases} \mathbf{H}^3(\Omega_\nu, \mathbb{R}^2) \rightarrow \mathbb{R} \\ v \mapsto \langle \rho(Dv) \rangle_N^2 - 2\langle \rho(Dv), \omega \rangle_N + \epsilon |v|_{\mathbf{H}^3(\Omega_\nu, \mathbb{R}^2)}^2. \end{cases}$$

The goal being to prove the existence/uniqueness of the solution of the introduced functional minimization problem, the functional  $\mathcal{J}_\epsilon$  is rephrased in terms of the bilinear form  $a$  and the linear form  $L$  defined hereafter.

$$a : \begin{cases} \mathbf{H}^3(\Omega_\nu, \mathbb{R}^2) \times \mathbf{H}^3(\Omega_\nu, \mathbb{R}^2) \rightarrow \mathbb{R} \\ (u, v) \mapsto \langle \rho(Du), \rho(Dv) \rangle_N + \epsilon (u, v)_{3, \Omega_\nu, \mathbb{R}^2}, \end{cases} \quad L : \begin{cases} \mathbf{H}^3(\Omega_\nu, \mathbb{R}^2) \rightarrow \mathbb{R} \\ v \mapsto \langle \rho(Dv), \omega \rangle_N \end{cases}.$$

with  $(u, v)_{3, \Omega_\nu, \mathbb{R}^2} = \sum_{|\alpha|=3} \int_{\Omega_\nu} \langle \partial^\alpha u, \partial^\alpha v \rangle_2 dx_1 dx_2$ .

The minimization problem thus becomes :

$$\begin{cases} \text{Search for } \sigma_\epsilon \in K \text{ such that} \\ \forall v \in K, a(\sigma_\epsilon, \sigma_\epsilon) - 2L(\sigma_\epsilon) \leq a(v, v) - 2L(v). \end{cases} \quad (3)$$

The mappings  $a$  and  $L$  are continuous, but the trouble is that the bilinear form  $a$  is not  $V$ -elliptic, which prevents us from applying Stampacchia's theorem [13] straightforwardly. To circumvent this issue, an artificial term is introduced in the minimization problem formulation as follows:

$$\begin{cases} \text{Search for } \sigma_\epsilon \in K \text{ such that} \\ \forall v \in K, a(\sigma_\epsilon, \sigma_\epsilon) - 2L(\sigma_\epsilon) + \|\beta(\sigma_\epsilon)\|_{2l}^2 \leq a(v, v) - 2L(v) + \|\beta(v)\|_{2l}^2. \end{cases} \quad (4)$$

This new phrasing involves the bilinear form denoted by  $\hat{a}$  defined by  $\hat{a} : \begin{cases} \mathbf{H}^3(\Omega_\nu, \mathbb{R}^2) \times \mathbf{H}^3(\Omega_\nu, \mathbb{R}^2) \rightarrow \mathbb{R} \\ (u, v) \mapsto a(u, v) + \langle \beta(u), \beta(v) \rangle_{2l} \end{cases}$  and the following propositions hold.

**Proposition 2.2.** *The mapping  $\|\hat{\cdot}\|$  defined on  $\mathbf{H}^3(\Omega_\nu, \mathbb{R}^2)$  by  $\|\hat{\cdot}\| : \begin{cases} \mathbf{H}^3(\Omega_\nu, \mathbb{R}^2) \rightarrow \mathbb{R} \\ v \mapsto \sqrt{\hat{a}(v, v)} \end{cases}$  is an Hilbertian norm.*

*Proof.* The proof is based on the argument of connectedness of  $\Omega_\nu$  and the property of  $P_1$ -unisolvence of the set  $A$ .  $\square$

**Proposition 2.3.** *The norm  $\|\hat{\cdot}\|$  is equivalent to the norm  $\|\cdot\|_{\mathbf{H}^3(\Omega_\nu, \mathbb{R}^2)}$  on  $\mathbf{H}^3(\Omega_\nu, \mathbb{R}^2)$ .*

*Proof.* The proof is based on a result of equivalence of norms by Nečas [14] and on the continuity of the bilinear form  $\hat{a}$  on  $\mathbf{H}^3(\Omega_\nu, \mathbb{R}^2) \times \mathbf{H}^3(\Omega_\nu, \mathbb{R}^2)$ .  $\square$

It results in the following theorem.

**Theorem 2.4.** *Problem (2) admits a unique solution  $\sigma_\epsilon \in K$ . This solution is characterized by the variational inequality  $\forall v \in K, \hat{a}(\sigma_\epsilon, v - \sigma_\epsilon) \geq L(v - \sigma_\epsilon)$ .*

*Proof.* The proof is based on Stampacchia theorem [13].  $\square$

## 2.2. Characterization of the solution

Let  $K_0$  be the vector subspace of  $\mathbf{H}^3(\Omega_\nu, \mathbb{R}^2)$  defined by  $K_0 = \{v \in \mathbf{H}^3(\Omega_\nu, \mathbb{R}^2) \mid \beta(v) = 0_{\mathbb{R}^{2l}}\}$ .

Let  $S$  be the set defined by  $S = \{u \in \mathbf{H}^3(\Omega_\nu, \mathbb{R}^2) \mid \forall v \in K_0, a(u, v) = L(v)\}$ .

Then the following proposition holds.

**Proposition 2.5.** *The unique solution  $\sigma_\epsilon$  of problem (2) is characterized by :  $\{\sigma_\epsilon\} = K \cap S$ .*

### 2.3. Lagrange multipliers

We now introduce Lagrange multipliers, which enables us to define the variational formulation of problem (2) on the whole space  $H^3(\Omega_\nu, \mathbb{R}^2)$  and to obtain a variational equality instead of a variational inequality. Let  $K_0^\perp$  be the orthogonal of  $K_0$  in  $V$  for the scalar product  $\widehat{a}(\cdot, \cdot)$ .

$$K_0^\perp = \{u \in H^3(\Omega_\nu, \mathbb{R}^2) \mid \widehat{a}(u, v) = 0, \forall v \in K_0\}.$$

The space  $V$  can be written as the direct sum  $V = K_0^\perp \oplus K_0$ .

Let  $\beta|_{K_0^\perp}$  be the restriction of  $\beta$  to  $K_0^\perp$ . Then  $\beta|_{K_0^\perp}$  is a topological isomorphism.

**Theorem 2.6.** *If  $\sigma_\epsilon$  is the unique solution of problem (2), then  $\sigma_\epsilon$  is also the solution of the following problem with Lagrange multipliers :*

$$\begin{cases} \text{Search for } (\sigma_\epsilon, \lambda) \in K \times \mathbb{R}^{2l}, \\ \forall v \in V, a(\sigma_\epsilon, v) - L(v) + \langle \lambda, \beta(v) \rangle_{2l} = 0. \end{cases} \quad (5)$$

### 2.4. Theoretical convergence result

Let  $D$  be a subset of  $\mathbb{R}^{+*}$  admitting 0 as accumulation point. For each  $d \in D$ , let  $A^d$  be a set of  $N = N(d)$  distinct points of  $\Omega_\nu$  containing a  $P^1$ -unisolvent subset.

We suppose that  $\sup_{x \in \Omega_\nu} \delta(x, A^d) = d$ , where  $\delta$  is the Euclidean distance in  $\mathbb{R}^2$ . Thus  $d$  is the radius of the largest sphere included in  $\Omega_\nu$  that contains no point from  $A^d$  (Hausdorff distance). Also,

$$\lim_{d \rightarrow 0} \sup_{x \in \Omega_\nu} \delta(x, A^d) = 0. \quad (6)$$

For all  $d \in D$ , we denote by  $\rho^d$  the mapping defined by :  $\rho^d : \begin{cases} H^2(\Omega_\nu, \mathbb{R}^{2 \times 2}) \rightarrow (\mathbb{R}^{2 \times 2})^{N(d)} \\ v \mapsto \rho^d(v) = ((v(a))_{a \in A^d})^T \end{cases}$ .

Then we introduce the norm  $\|\widehat{\cdot}\|_d$  equivalent to the norm  $\|\cdot\|_{H^3(\Omega_\nu, \mathbb{R}^2)}$  on  $H^3(\Omega_\nu, \mathbb{R}^2)$  defined by:  $\forall v \in H^3(\Omega_\nu, \mathbb{R}^2)$ ,

$$\|\widehat{v}\|_d = [ \langle \rho^d(Dv) \rangle_{N(d)}^2 + \epsilon |v|_{H^3(\Omega_\nu, \mathbb{R}^2)}^2 + \|\beta(v)\|_{2l}^2 ]^{\frac{1}{2}}.$$

The following theorem holds :

**Theorem 2.7.** *Suppose that there exists a function  $\widehat{f} \in K$  such that for all  $d \in D$ :  $\rho^d(D\widehat{f}) = \omega$ , and  $\epsilon = \epsilon(d) \in ]0, \epsilon_0]$ ,  $\epsilon_0 > 0$ .*

*For all  $d \in D$ , we denote by  $\sigma_\epsilon^d$  the unique solution of problem (2), then under the above assumptions we have:*

$$\lim_{d \rightarrow 0} \|\sigma_\epsilon^d - \widehat{f}\|_{H^3(\Omega_\nu, \mathbb{R}^2)} = 0. \quad (7)$$

### 2.5. Discretization

We now discretize the variational problem (5). Let  $\mathcal{H}$  be an open bounded subset of  $\mathbb{R}^{+*}$  admitting 0 as accumulation point. Let us recall that the elements of class  $\mathcal{C}^{k'}$  can be used for the computation of discrete  $D^m$ -splines (in our case  $m = 3$ ) with  $m \leq k' + 1$ . Consequently,  $(k', m) = (2, 3)$  is a satisfactory combination. We also recall that for all  $n \in \mathbb{N}$  and for all subset  $E$  of  $\mathbb{R}^2$ ,  $Q_l(E)$  denotes the space of the restrictions to  $E$  of the polynomial functions over  $\mathbb{R}^2$  of degree  $\leq l$  with respect to each variable.  $\forall h \in \mathcal{H}$ , let  $(V_h)^2$  be the subspace of  $H^3(\Omega_\nu, \mathbb{R}^2)$  of finite dimension with  $(V_h)^2 \subset C^1(\overline{\Omega_\nu}, \mathbb{R}^2)$ . The reference finite element is the Bogner-Fox-Schmit  $\mathcal{C}^2$  rectangle (cf. [15]). It is defined as the following triple  $(K, P_K, \Sigma_K)$ :

- Let  $b_{00} = (b_{00}^1, b_{00}^2) \in \mathbb{R}^2$ ,  $h_1, h_2 > 0$ .  $K \subset \Omega_\nu$  is the rectangle with vertices  $b_\beta = b_{00} + \gamma_1 h_1 \vec{e}_1 + \gamma_2 h_2 \vec{e}_2$  with  $\gamma = (\gamma_1, \gamma_2) \in \mathbb{N}^2$  such that  $0 \leq \gamma_1 \leq 1$  and  $0 \leq \gamma_2 \leq 1$ , and  $(\vec{e}_1, \vec{e}_2)$  the canonical basis of  $\mathbb{R}^2$ .
- $P_K = Q_5(K)$ .
- The set of linear mappings  $\Sigma_K$  is defined by:  $\Sigma_K = \{v \mapsto \partial^\alpha v(b_\gamma) \mid |\alpha|_\infty \leq 2\}$ , where, if  $\alpha = (\alpha_1, \alpha_2)$ ,  $|\alpha|_\infty = \max(\alpha_1, \alpha_2)$ .

The number of degrees of freedom of the Bogner-Fox-Schmit rectangle of class  $\mathcal{C}^2$  is thus equal to 36.

The basis functions are defined by  $p_\alpha^\gamma(x_1, x_2) = h_1^{\alpha_1} h_2^{\alpha_2} q_{\alpha_1}^{\gamma_1} \left( \frac{x_1 - b_{00}^1}{h_1} \right) q_{\alpha_2}^{\gamma_2} \left( \frac{x_2 - b_{00}^2}{h_2} \right)$  with:

$$\begin{aligned} q_0^0(t) &= (1-t)^3(6t^2+3t+1), & q_1^0(t) &= t(1-t)^3(3t+1), & q_2^0(t) &= \frac{1}{2}t^2(1-t)^3 \\ q_0^1(t) &= t^3(6t^2-15t+10), & q_1^1(t) &= t^3(1-t)(3t-4), & q_2^1(t) &= \frac{1}{2}t^3(t-1)^2. \end{aligned}$$

We can prove that problem (5) is decoupled with respect to each component. Let  $(v_q)_{q=1,2}$  be the components of  $v \in \mathbb{H}^3(\Omega_\nu, \mathbb{R}^2)$ ,  $((\omega_q^i)^T)_{q=1,2}$  the  $q^{\text{th}}$  row of  $\omega_i$ ,  $\forall i \in \{1, \dots, N\}$ , and  $\lambda = (\lambda^q)_{q=1,2}$  with  $\lambda^q \in \mathbb{R}^l$ .

Problem (5) can therefore be stated by:

$$\left\{ \begin{array}{l} \text{Search for } (\sigma_\epsilon = (\sigma_\epsilon^q)_{q=1,2}, \lambda = (\lambda^q)_{q=1,2}) \in \mathbb{H}^3(\Omega_\nu, \mathbb{R}^2) \times \mathbb{R}^{2l} \text{ such that} \\ \sigma_\epsilon \in K, \\ \forall v = (v^q)_{q=1,2} \in \mathbb{H}^3(\Omega_\nu, \mathbb{R}^2), \forall q \in \{1, 2\}, \\ \sum_{i=1}^N \langle \nabla \sigma_\epsilon^q(a_i), \nabla v^q(a_i) \rangle_2 + \epsilon (\sigma_\epsilon^q, v^q)_{3, \Omega_\nu, \mathbb{R}} + \sum_{i=1}^l \lambda_i^q v^q(b_i) = \sum_{i=1}^N \langle \nabla v^q(a_i), \omega_q^i \rangle_2. \end{array} \right. \quad (8)$$

We solve (8) in  $V_h$  for  $q = 1, 2$ . Let  $M_h$  be the dimension of  $V_h$  and  $\{P_j^h\}_{j=1, \dots, M_h}$  be basis functions (for the sake of clarity, from now on, we use this notation for the basis functions). We denote by  $(\sigma_\epsilon^{h,q})_{q=1,2}$  the approximate solution of (8) in  $(V_h)^2$ ;  $\sigma_\epsilon^{h,q}$  is decomposed into the basis  $\{P_j^h\}_{j=1, \dots, M_h}$  as follows:

$$\left\{ \begin{array}{l} \forall q = 1, 2, \\ \exists (\alpha_j^q)_{j=1, \dots, M_h} \in \mathbb{R} \text{ such that } \sigma_\epsilon^{h,q} = \sum_{j=1}^{M_h} \alpha_j^q P_j^h. \end{array} \right. \quad (9)$$

For  $q = 1, 2$ , taking successively  $v^q = P_k^h$ ,  $k = 1, \dots, M_h$  in (8), the studied problem becomes:

$$\left\{ \begin{array}{l} \text{Search for } \alpha^q \in \mathbb{R}^{M_h} \text{ such that} \\ \sum_{i=1}^{M_h} \alpha_i^q P_i^h(b_j) = \eta_j^q, \forall j \in \{1, \dots, l\}, \forall k = 1, \dots, M_h, \\ \sum_{i=1}^N \sum_{j=1}^{M_h} \alpha_j^q \langle \nabla P_j^h(a_i), \nabla P_k^h(a_i) \rangle_2 + \epsilon \sum_{j=1}^{M_h} \alpha_j^q (P_j^h, P_k^h)_{3, \Omega_\nu, \mathbb{R}} - \sum_{i=1}^N \langle \nabla P_k^h(a_i), \omega_q^i \rangle_2 + \sum_{i=1}^l \lambda_i^q P_k^h(b_i) = 0. \end{array} \right. \quad (10)$$

The numerical problem boils down to the resolution of two decoupled sparse linear systems of dimension  $(M_h + l) \times (M_h + l)$  which can be written by means of matrices  $A^h$ ,  $B^h$  and  $R^h$ ,

$$A^h = \left( \frac{\partial P_j^h}{\partial x_1}(a_i) \right)_{\substack{1 \leq i \leq N, \\ 1 \leq j \leq M_h}}, \quad B^h = \left( \frac{\partial P_j^h}{\partial x_2}(a_i) \right)_{\substack{1 \leq i \leq N, \\ 1 \leq j \leq M_h}} \in (\mathcal{M}_{N \times M_h}(\mathbb{R}))^2,$$

$$R^h = \left( (P_j^h, P_i^h)_{3, \Omega_\nu, \mathbb{R}} \right)_{1 \leq i \leq M_h, 1 \leq j \leq M_h} \in \mathcal{M}_{M_h \times M_h}(\mathbb{R}).$$

Both systems are written in the following way:

$$\left\{ \begin{array}{l} ((A^h)^T A^h + (B^h)^T B^h + \epsilon R) \alpha^q + (P^h)^T \lambda^q = \xi_q, \\ \text{with } P^h \alpha^q = \eta^q, \forall q \in \{1, 2\}, \end{array} \right. \quad (11)$$

where  $P^h = (P_j^h(b_i))_{\substack{1 \leq i \leq l, \\ 1 \leq j \leq M_h}} \in \mathcal{M}_{l \times M_h}(\mathbb{R})$  and  $\xi_q = \left( \sum_{i=1}^N \langle \nabla P_k^h(a_i), \omega_q^i \rangle_2 \right)_{1 \leq k \leq M_h}$ . We group the unknown  $\alpha^q$  and  $\lambda^q$  in a single unknown vector, and we write the system as a matrix equation of the form:

$$\begin{array}{c}
 M_h \\
 \left( \begin{array}{c|c}
 (A^h)^T A^h + (B^h)^T B^h + \epsilon R & (P^h)^T \\
 \hline
 P^h & 0
 \end{array} \right)
 \begin{array}{c}
 l \\
 \left( \begin{array}{c}
 \alpha^q \\
 \lambda^q
 \end{array} \right)
 =
 \begin{array}{c}
 \xi^q \\
 \eta^q
 \end{array}
 \end{array}
 \end{array}$$

$\underbrace{\hspace{10em}}_{\kappa^h}$

**Remark 2.8.** A result of convergence analogous to the one in Theorem 2.7 can be obtained in the discrete setting.

**Remark 2.9.** The matrix  $\kappa^h$  of the system is symmetric indefinite.

**Remark 2.10.** In practice, the interpolation conditions are set on the boundary nodes of the finite element mesh. In this case, we have the following result:

**Proposition 2.11.** *Matrix  $\kappa^h$  is nonsingular.*

In our application, to solve the considered linear system, we use the diagonal pivoting method due to Bunch and Parlett [16] which computes a permutation  $P$  such that  $PAP^T = LDL^T$  - when solving a linear system whose symmetric definite matrix is  $A$ , where  $D$  is a direct sum of 1 by 1 and 2 by 2 pivot blocks and  $L$  is unit lower triangular (see also [17]).  $P$  is chosen so that the entries in the unit lower triangular  $L$  satisfy  $|l_{ij}| \leq 1$ . This factorization involves  $\frac{n^3}{3}$  flops and once computed can be used to solve  $Ax = b$  with  $\mathcal{O}(n^2)$  work.

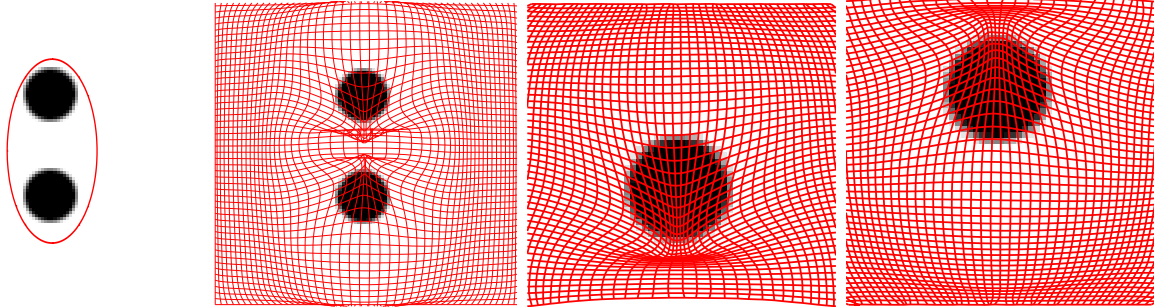
### 3. NUMERICAL EXPERIMENTS

In the sequel, we provide numerical simulations. Classically, in the  $D^m$ -spline setting, parameter  $\epsilon$  balancing the semi-norm is set to  $10^{-6}$ . (There also exist methods for an automatic choice of  $\epsilon$  mainly based on statistical considerations as the generalized cross-validation and the generalized maximum likelihood methods (see [18] and [19]). Owing to the fact that the proposed algorithm calls basic linear algebra functions such that transposing matrices, summing matrices, multiplying matrices or solving linear systems, it appeared relevant to use LAPACK and Basic Linear Algebra Subprogram routines. BLAS is a corpus of routines that provide standard building blocks for performing basic vector and matrix operations. LAPACK (designed at the outset to exploit BLAS routines) provides routines for solving systems of linear equations among others. For each subdomain  $\Omega_\nu$ ,  $\nu \in \{1, \dots, \mathcal{N}\}$ , we obtain two disconnected linear systems to be solved with the same matrix. Our resorting to BLAS/LAPACK thus seems apposite. The computations on each subdomain  $\Omega_\nu$  being independent, the use of OpenMP appeared relevant. The OpenMP Application Program Interface supports multi-platform shared-memory programming in C/C++ and Fortran on all architectures (see the official website <http://openmp.org/wp/>).

The first application involving large deformations is provided in Fig. 2 and is similar to an application given in [20] in the case of topology-preserving segmentation. The synthetic Reference image represents two disks. The Template image, which is defined on the same image domain ( $100 \times 100$ ), is made of a black ellipse such that when superimposed on the Reference image its boundary encloses the two disks (see Fig. 2 (a)). The application of the combined segmentation-registration process alone yields two regions exhibiting overlaps (Fig. 2(b)): the upper part of the image including the upper disk (size  $50 \times 50$ ) and the lower part of the image containing the lower disk (size  $50 \times 50$ ). We thus propose to apply our proposed algorithm on each region independently,



the upper region being triangulated by means of 10 rectangles in direction  $x$  and 10 rectangles in direction  $y$ , similarly for the lower region. The computational time drops to 0.52 second, which means a depletion by a factor 6.9 in comparison to the computational time inherent to the application of the method [9] on the whole domain. This optimal computational time is obtained with the following requests: MKL\_NUM\_THREADS=6 and OMP\_NUM\_THREADS=2. We display the obtained topology-preserving deformation fields together with the values of the discrete Jacobians in Fig. 2 (c) and Fig. 2 (d).



(A) Reference image and boundary of the ellipse constituting the Template image superimposed. (B) Obtained global deformation field when topology preservation is not enforced. (C) Corrected first region:  $\min(J_{ff}) = 0.06$ ,  $\min(J_{fb}) = 0.08$ ,  $\min(J_{bf}) = 0.09$  and  $\min(J_{bb}) = 0.11$ . (D) Corrected second region:  $\min(J_{ff}) = 0.33$ ,  $\min(J_{fb}) = 0.31$ ,  $\min(J_{bf}) = 0.35$  and  $\min(J_{bb}) = 0.29$ .

FIGURE 2. Example of the disks.

In another application, the goal is to map a disk to a slice of the brain (courtesy of the Laboratory Of Neuro-Imaging, school of Medicine, University of California) defined on the same image domain (size  $120 \times 190$ ), while preserving topology (see Fig. 3). When applying the combined segmentation/registration model developed in [20] without regriding steps, we obtain a deformation field exhibiting two regions with overlaps as depicted in Fig. 4(b) and Fig. 4(c).

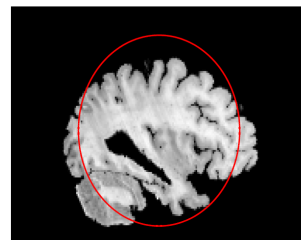
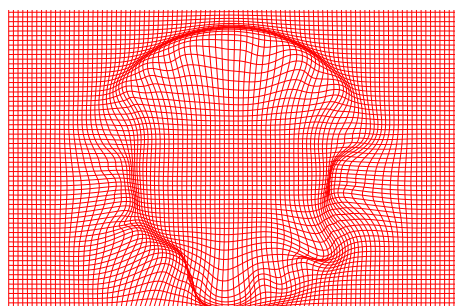
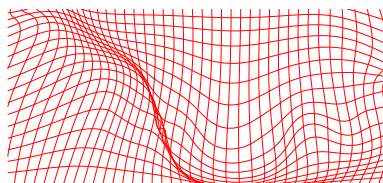


FIGURE 3. Reference image and boundary (in red) of the disk constituting the Template image.

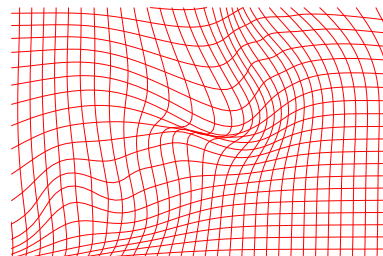
If we merely apply the method developed in [9] (which consists in applying the correction/reconstruction algorithm on the whole image domain with global condition on the deformation component means), the execution time reaches 50.9 seconds (the domain being triangulated by means of 19 rectangles in direction  $x$  and 12 rectangles in direction  $y$  - with 9 basis functions per node, it results in two linear systems (one for each component of the deformation field) of size  $2341 \times 2341$  to be solved-). By applying our proposed method (which signifies: concentrating the computational effort on the two regions exhibiting twists- the first one of size  $30 \times 30$  triangulated by means of 6 rectangles in direction  $x$  and 6 rectangles in direction  $y$  and the second one of size  $80 \times 40$  triangulated by means of 10 rectangles in direction  $x$  and 10 rectangles in direction  $y$  -, equipping the two subproblems with Lagrange interpolation conditions and parallelizing the code), the computational time drops to 0.63 second, which means a depletion by a factor 80. For our configuration, the maximal number of threads is equal to 12 and the optimal computational time is obtained with the following requests: MKL\_NUM\_THREADS=6 and OMP\_NUM\_THREADS=2. We display the obtained topology-preserving deformation fields together with the values of the discrete Jacobians in Fig. 4(e) and 4(f).



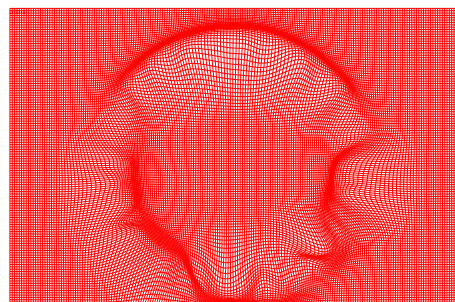
(A) Obtained global deformation field when topology preservation is not enforced.



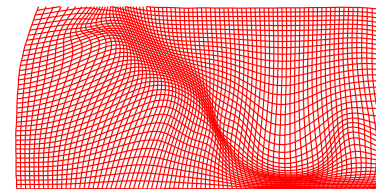
(B) Zoom on the first region exhibiting twists.



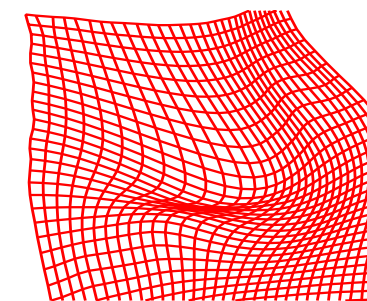
(C) Zoom on the second region exhibiting overlaps



(D) Global obtained deformation field after correction.



(E) Zoom on the corrected first region:  
 $\min(J_{ff}) = 0.20$ ,  $\min(J_{fb}) = 0.21$ ,  
 $\min(J_{bf}) = 0.17$  and  $\min(J_{bb}) = 0.19$ .



(F) Zoom on the corrected second region:  
 $\min(J_{ff}) = 0.13$ ,  $\min(J_{fb}) = 0.19$ ,  
 $\min(J_{bf}) = 0.21$  and  $\min(J_{bb}) = 0.23$ .

FIGURE 4. Example of the slice of the brain: uncorrected deformation field and orientation-preserving deformation field after correction.

## CONCLUSION

To conclude, the obtained results are satisfactory, and less memory and time-consuming than a regriding method.

Let us emphasize that the focus of the paper is on the mathematical presentation and well-posedness of the method. Hence, the computational results are currently still restricted to two dimensions. Nevertheless, from a mathematical point of view, the first stage of the algorithm can be extended to the 3D case and all the stated results (in the reconstruction stage) hold in three dimensions. The main brake to the straight extension to 3D is the phase of identification of subdomains where the computations need to be done. The semi-automation of this process, based on segmentation techniques, is a work in progress.

## REFERENCES

- [1] J. Ashburner, P. Neelin, D. L. Collins, A. Evans, and K. J. Friston, "Incorporating prior knowledge into image registration," *Neuroimage*, vol. 6, no. 4, pp. 344–352, 1997.
- [2] J. Ashburner, J. L. R. Andersson, and K. J. Friston, "High-dimensional image registration using symmetric priors," *Neuroimage*, vol. 9, no. 6, pp. 619–628, 1999.
- [3] J. Ashburner and K. J. Friston, "Voxel-based morphometry: the methods," *Neuroimage*, vol. 11, no. 6, pp. 805–821, 2000.
- [4] O. Musse, F. Heitz, and J.-P. Armspach, "Topology preserving deformable image matching using constrained hierarchical parametric models," *IEEE Trans. Image Process.*, vol. 10, no. 7, pp. 1081–1093, 2001.
- [5] V. Noblet, C. Heinrich, F. Heitz, and J.-P. Armspach, "3-D deformable image registration: a topology preservation scheme based on hierarchical deformation models and interval analysis optimization," *IEEE Trans. Image Process.*, vol. 14, no. 5, pp. 553–566, 2005.
- [6] E. Haber and J. Modersitzki, "Numerical methods for volume preserving image registration," *Inverse Probl.*, vol. 20, pp. 1621–1638, October 2004.
- [7] E. Haber and J. Modersitzki, "Image registration method with guaranteed displacement regularity," *Int. J. Comput. Vision*, vol. 71, pp. 361–372, March 2007.
- [8] G. E. Christensen, R. Rabitt, and M. I. Miller, "Deformable templates using large deformation kinematics," *IEEE Trans. Imag. Process.*, vol. 10, pp. 1435–1447, October 1996.
- [9] C. Le Guyader, D. Apprato, and C. Gout, "On the construction of topology-preserving deformation fields," *IEEE Transactions on Image Processing*, vol. 21, no. 4, pp. 1587–1599, 2012.
- [10] B. Karaçali and C. Davatzikos, "Estimating topology preserving and smooth displacement fields," *IEEE Trans. Med. Imag.*, vol. 23, pp. 868–880, July 2004.
- [11] R. Arcangéli, M. López de Silanes, and J. Torrens, *Multidimensional minimizing splines. Theory and applications*. Boston, MA: Grenoble Sciences, Kluwer Academic Publishers, 2004.
- [12] R. A. Adams, *Sobolev Spaces*. Boston, MA: Academic, 1975.
- [13] H. Brezis, *Analyse fonctionnelle. Théorie et Applications*. Paris: Dunod, 2005.
- [14] J. Nečas, *Les méthodes directes en théorie des équations elliptiques*. Paris: Masson, 1967.
- [15] P. G. Ciarlet, *The Finite Element Method for Elliptic Problems*. Amsterdam, The Netherlands: North Holland, 1978.
- [16] J. R. Bunch and B. N. Parlett, "Direct methods for solving symmetric indefinite systems of linear equations," *SIAM J. Numer. Anal.*, vol. 8, pp. 639–655, 1971.
- [17] G. H. Golub and C. F. Van Loan, *Matrix Computations, 4<sup>th</sup> edition*. Baltimore: Johns Hopkins University Press, 2013.
- [18] P. Craven and G. Wahba, "Smoothing noisy data with spline functions," *Numer. Math.*, vol. 31, pp. 377–403, 1979.
- [19] C. Gu and G. Wahba, "Minimizing GCV/GML scores with multiple smoothing parameters via the newton method," *SIAM Journal on Scientific and Statistical Computing*, vol. 12, no. 2, pp. 383–398, 1991.
- [20] C. Le Guyader and L. Vese, "A combined segmentation and registration framework with a nonlinear elasticity smoother," *Computer Vision and Image Understanding*, vol. 115, no. 12, pp. 1689–1709, 2011.